

UDC 681.7

Method for Detecting Small Aerial Objects Appearing in Field of View in Controlled Part of Celestial Sphere in Infrared Range

Agayev F. G., Asadov H. H., Aliyeva G. V.

National Aerospace Agency, Baku, Republic of Azerbaijan

E-mail: hikmetasadov88@gmail.com

The article is devoted to the developed method of infrared detection of group remote high-temperature objects. The problem of searching for the extremum of the total infrared radiation of a group of non-identical thermal objects carrying out a group flight is formulated and solved using the variational optimization method. Examples of such objects include the flight of aircraft in a group, ground scenes involving a group of objects of interest, temperature diagnostics of various points of buildings, control of automobile traffic on highways, control of group flights of birds, drones, etc. A condition has been determined under which the total value of the infrared radiation flux of thermal elements in the group reaches an extreme value. The regression relationship function between the emission coefficient of the thermal elements of the group and the atmospheric transmission coefficient has been calculated. The problem of optimal control of small thermal objects randomly distributed in the atmosphere is practically solved using a ground-based multi-radar system in which elements of a multi-radar system monitor flying objects with different values of the radiation coefficient on the routes and different atmospheric transparencies. The proposed method can be used for remote control of flight or the functioning of a group of flying thermal objects with different values of the radiation coefficient with a special procedure for selecting a controlled aircraft for observation by an element of a multi-radar system. The property of the extremum of the total IR radiation flux was found in the inverse relationship between the radiation coefficients of all controlled flying objects and the transparency of the atmosphere along the route between the multi-radar element and the controlled flying object.

Keywords: temperature measurements; group flight; atmosphere; atmospheric transparency

DOI: [10.20535/RADAP.2024.97.76-81](https://doi.org/10.20535/RADAP.2024.97.76-81)

Introduction

It is well known that any object with a temperature above zero Kelvin emits infrared radiation [1]. At the same time, infrared (IR) radiation makes it possible to study both moving and non-moving objects emitting in the thermal range [2]. Infrared object detection is one of the methods of remote sensing of the surrounding world and is widely used for both civilian and military purposes [3]. Infrared object detection can in principle be used to detect objects at both close and long distances.

Infrared measurement at close distances is used in medicine [4–7], veterinary medicine [8–11], in the study of technological processes [12–14], in the construction of buildings [15–17], etc. At the same time, objects of interest often exist in the form of a certain group of thermal emitters and a general qualitative characteristic of the functioning of such groups can be given using such an indicator as the total IR radiation of elements of such groups. As examples of such objects, it is possible to show flights of aircraft in a group.

For example, in [18], single-position and multi-position methods for detecting small aerial objects using computational methods to determine secondary radiation fluxes emanating from these objects are considered.

In [19], the advantages of IR radar systems such as a wide range of radio frequencies and the ability to quickly process primary results compared with microwave radars are noted. IR radars are also more resistant to various atmospheric influences compared to microwave radars.

According to [20], automatic detection and tracking of small flying objects with possible atmospheric noise is possible by determining individual structural elements according to set values of the signal-to-noise ratio. Further application of genetic algorithms makes it possible to increase the reliability of detecting such objects.

As noted in [21], the IR detection of small flying objects in the marine environment encounters the problem of a small signal-to-noise ratio of the extracted useful signal. At the same time, both empirical models

and statistical analysis methods should be used to take into account the influence of marine environmental factors.

The work [22] reports on the use of multi-radar, multi-sensor systems consisting of a warning and decision-making system and a system for generating aviation weather information designed to detect and predict a non-flight weather situation (the appearance of tornadoes, lightning, etc.).

According to [23], the use of a “gray” morphological filter will enhance the useful signal and weaken the influence of the background during IR detection of small flying objects. In this case, the desired small objects can be redone according to the algorithm of the maximum local sum. According to [24], drone detection can be effectively implemented by combining the use of IR radars, acoustic sensors and computer images.

Obviously, the detection of thermal sources must be calibrated in one way or another, and the quality of such operations is often determined by the signal-to-noise ratio in the measuring result. Therefore, the researcher is always interested in getting the best result with low total noise. The specified property of remote measurements actualizes the formation of various optimization tasks related to remote thermal detection.

1 Materials and methods

Next, we will specifically focus on conducting group thermal detection of objects and for this reason we will provide some basic information about the radiation and re-radiation of remote celestial objects borrowed from the source [25]. When considering the case of the infrared radiation flux of one object using an infrared camera (Fig. 1), the total radiation at the camera input can be estimated using the following expression:

$$W_{tot} = E_{obj} + E_{refl} + E_{atm} + E_{ph}, \quad (1)$$

where E_{obj} is the radiation of the object of interest to us; E_{refl} is the re-reflected radiation of the environment; E_{atm} is the radiation of the atmosphere; E_{ph} is background radiation.

These components are determined by the following expressions:

$$E_{obj} = \varepsilon_{obj} \cdot \tau_{atm} \cdot \sigma(T_{obj})^4, \quad (2)$$

where ε_{obj} is the radiation coefficient of the object; σ is the Stefan-Boltzmann constant; τ_{atm} is the transmission of the atmosphere; T_{obj} is the temperature of the atmosphere;

$$E_{refl} = \rho_{obj} \cdot \tau_{atm} \cdot \sigma(T_{refl})^4 = (1 - \varepsilon_{obj}) \cdot \tau_{atm} \cdot \sigma(T_{refl})^4, \quad (3)$$

where ρ_{obj} is the spectral reflection coefficient; T_{refl} is the reflected temperature;

$$E_{atm} = \varepsilon_{atm} \cdot \sigma(T_{atm})^4 = (1 - \tau_{atm}) \cdot \sigma(T_{atm})^4, \quad (4)$$

where ε_{atm} is the radiation coefficient of the atmosphere; T_{atm} is the temperature of the atmosphere;

$$E_{ph} = \sigma(T_{ph})^4, \quad (5)$$

where T_{ph} is the background temperature.

Taking into account the expressions (2)-(5) we obtain the following expression for the total heat flow

$$W_{tot} = \varepsilon_{obj} \tau_{atm} \sigma(T_{obj})^4 + (1 - \varepsilon_{obj}) \tau_{atm} \sigma(T_{refl})^4 + (1 - \tau_{atm}) \sigma(T_{atm})^4 + \sigma(T_{ph})^4. \quad (6)$$

Next, we introduce the following interrelation function:

$$\varepsilon_{obj} = \varepsilon(\tau_{atm})$$

and the ordered set

$$T = \{\tau_{atm.i}\}; \quad i = \overline{1, n},$$

where $(\tau_{atm.i} - \tau_{atm.i-1}) = \Delta\tau_{atm}$; $\Delta\tau_{atm} = const.$

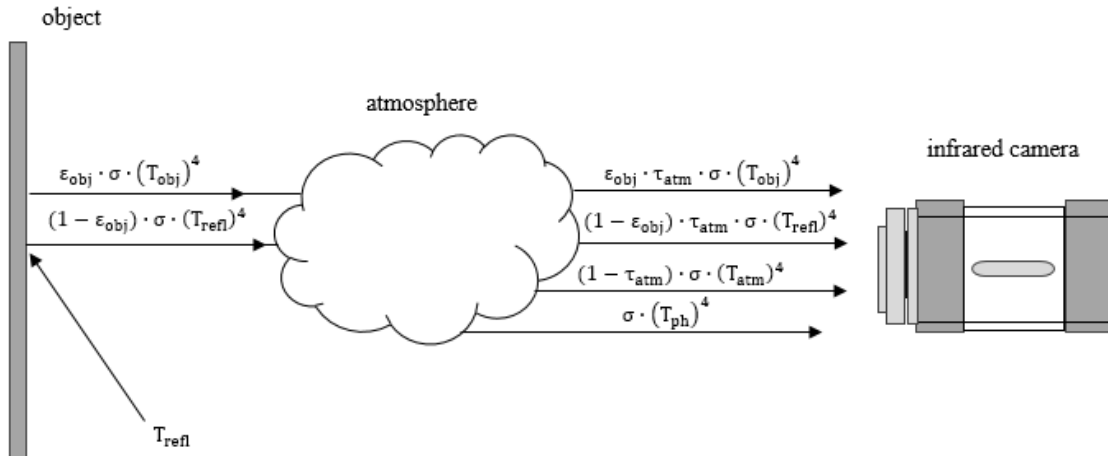


Fig. 1. The total optical radiation at the input of the infrared camera, formed as the sum of four components (1)

From expression (6) we get

$$\frac{W_{tot}}{\sigma \varepsilon_{obj} \tau_{atm}} = a_1 + \frac{a_2}{\varepsilon_{obj} \tau_{atm}} + \frac{a_3}{\varepsilon_{obj}}, \quad (7)$$

where

$$\left. \begin{aligned} a_1 &= (T_{obj}^4 - T_{relf}^4) \\ a_2 &= (T_{atm}^4 + T_{ph}^4) \\ a_3 &= (T_{relf}^4 - T_{atm}^4) \end{aligned} \right\} \quad (8)$$

based on the expression (7), we will make the corresponding sum for all $i = (1, n)$.

$$\begin{aligned} & \frac{1}{\sigma} \sum_{i=1}^n \frac{W_{tot}}{\varepsilon_{obj}(\tau_{atm,i}) \tau_{atm,i}} = \\ & = \sum_{i=1}^n \left[a_1 + \frac{a_2}{\varepsilon_{obj}(\tau_{atm,i}) \tau_{atm,i}} + \frac{a_3}{\varepsilon_{obj}(\tau_{atm,i})} \right]. \quad (9) \end{aligned}$$

In this case, we have $W_{tot} = W_{tot}(\varepsilon(\tau_{atm,i}))$, i.e. the total measured signal depends on the choice of the type of function $\varepsilon(\tau_{atm,i})$. Turning to the continuous form of writing, we write expression (9) as

$$\begin{aligned} & \frac{1}{\sigma} \int_0^{\tau_{atm,max}} \frac{W_{tot}(\varepsilon(\tau_{atm}))}{\varepsilon_{obj}(\tau_{atm}) \tau_{atm}} d\tau_{atm} = \\ & = \int_0^{\tau_{atm,max}} \left[a_1 + \frac{a_2}{\varepsilon_{obj}(\tau_{atm}) \tau_{atm}} + \frac{a_3}{\varepsilon_{obj}(\tau_{atm})} \right] d\tau_{atm}. \quad (10) \end{aligned}$$

Let's impose the following restriction on the interrelation function (9)

$$\int_0^{\tau_{atm,max}} \varepsilon(\tau_{atm}) d\tau_{atm} = C; \quad C = const. \quad (11)$$

Taking into account expressions (10) and (11), two target functions F_1 and F_2 can be formed using the method of unconditional variational optimization, where

$$\begin{aligned} F_1 &= \frac{1}{\sigma} \int_0^{\tau_{atm,max}} \frac{W_{tot}(\varepsilon(\tau_{atm}))}{\varepsilon_{obj}(\tau_{atm}) \tau_{atm}} d\tau_{atm} + \\ & + \lambda_1 \left[\int_0^{\tau_{atm,max}} \varepsilon_{obj}(\tau_{atm}) d\tau_{atm} - C \right], \quad (12) \end{aligned}$$

where λ_1 is the Lagrange multiplier;

$$\begin{aligned} F_2 &= \\ & = \int_0^{\tau_{atm,max}} \left[a_1 + \frac{a_2}{\varepsilon_{obj}(\tau_{atm}) \tau_{atm}} + \frac{a_3}{\varepsilon_{obj}(\tau_{atm})} \right] \times \\ & \times d\tau_{atm} + \lambda_2 \left[\int_0^{\tau_{atm,max}} \varepsilon(\tau_{atm}) d\tau_{atm} - C \right], \quad (13) \end{aligned}$$

where λ_2 is the Lagrange multiplier.

Because of the implicit form of the function $W_{tot}(\varepsilon(\tau_{atm}))$ next, we consider the solution of the optimization problem (13).

It is known from the theory of calculus of variations that the optimal function leading to the extremum F_2 must correspond to the condition

$$\frac{d \left\{ a_1 + \frac{a_2}{\varepsilon_{obj}(\tau_{atm}) \tau_{atm}} + \frac{a_3}{\varepsilon_{obj}(\tau_{atm})} + \lambda_2 \varepsilon_{obj}(\tau_{atm}) \right\}}{d\varepsilon_{obj}(\tau_{atm})} = 0. \quad (14)$$

From the condition (14) we get

$$-\frac{a_2}{\varepsilon_{obj}(\tau_{atm})^2 \tau_{atm}} - \frac{a_3}{\varepsilon_{obj}(\tau_{atm})^2} + \lambda_2 = 0. \quad (15)$$

From expression (15) we get

$$-\frac{1}{\varepsilon_{obj}(\tau_{atm})^2} \left[\frac{a_2}{\tau_{atm}} + a_3 \right] = -\lambda_2. \quad (16)$$

From expression (16) we find:

$$\varepsilon_{obj}(\tau_{atm}) = \sqrt{\frac{\frac{a_2}{\tau_{atm}} + a_3}{\lambda_2}}. \quad (17)$$

Thus, when solving (17), the functional (13) reaches an extremum.

2 Discussion

To find out the type of extremum of the functional F_2 , it is enough to take the derivative of expression (15) for the desired function and make sure that the result is always a positive value. Therefore, when solving (17), both functional (13) and functional (12) reach a minimum.

To calculate the Lagrange multiplier λ_2 , you can use expressions (11) and (17). Inserting expression (17) into (11) we get

$$\frac{1}{\sqrt{\lambda_2}} \int_0^{\tau_{atm,max}} \sqrt{\frac{a_2}{\tau_{atm}} + a_3} d\tau_{atm} = C. \quad (18)$$

Taking into account the expression (18), we find

$$\lambda_2 = \left[\frac{1}{C} \int_0^{\tau_{atm,max}} \sqrt{\frac{a_2}{\tau_{atm}} + a_3} d\tau_{atm} \right]^2. \quad (19)$$

Taking into account expressions (17) and (19), we finally obtain:

$$\varepsilon_{obj}(\tau_{atm}) = \frac{C \sqrt{\frac{a_2}{\tau_{atm}} + a_3}}{\int_0^{\tau_{atm,max}} \sqrt{\frac{a_2}{\tau_{atm}} + a_3} d\tau_{atm}}. \quad (20)$$

Based on the above, we can propose the following multi-radar technique for confirming the appearance in the field of view of an IR radar of the same type of thermal objects with a radiation coefficient $\varepsilon_{obj}(i)$ at a distance $L(i)$ equivalent to the optical thickness $\tau_{atm}(i)$, where i is the ordinal object number.

To implement the proposed method for detecting a group of flying thermal objects in a controlled area of the celestial sphere, a multi-radar system should be used, automatically rebuilt using guidance systems in

such a way that the ratio (17) between ε_{obj} and τ_{atm} are ensured.

The measuring and computing unit of the multi-radar system, with which the values of F_{1g} and F_{2g} are calculated, must track the changes in the following discrete sum

$$F_{1g} = \frac{1}{\sigma} \sum_{i=1}^n \frac{W_{tot}(i)}{\varepsilon_{obj}(\tau_{atm,i})\tau_{atm,i}}. \quad (21)$$

The extremum detection unit, with some kind of communication function, should provide detection of the minimum F_{1g} , which is equivalent to detecting a group of flying objects.

The block diagram of such a multi-radar system is conventionally shown in Fig. 2.

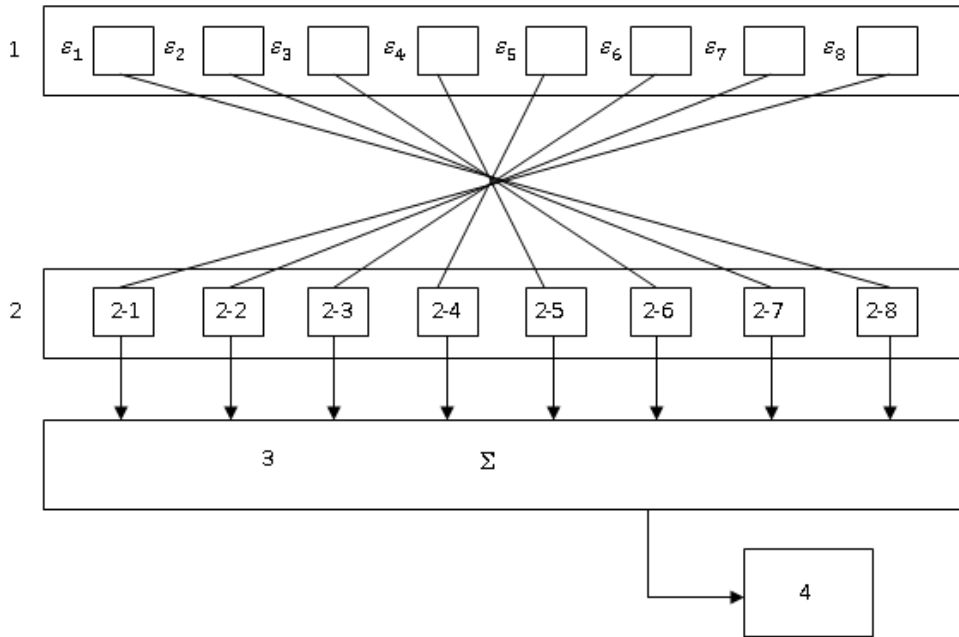


Fig. 2. The block diagram of the proposed multi-radar system for detecting groups of flying objects: 1 – group of detectable objects; 2 – group of IR radars; 3 – radar signals adder; 4 – minimum detector

3 Model researches

Taking into account the obtained solutions (17) and (20), we will conduct model studies, approximating the obtained solutions in the first approximation by the following functions satisfying the restrictive condition (11)

$$\varepsilon_{obj,1} = \varepsilon_0 - k\tau_{atm}, \quad (22)$$

$$\varepsilon_{obj,2} = k\tau_{atm}. \quad (23)$$

The graphical representation of the function (22) and (23) are shown in Fig. 3.

Since the model function (22) is more similar in nature to the obtained solutions (17) and (20), the value of the integrand in the first integral of expression (13) for function (22) should be less than for the model function (23).

The above integrand γ has the form

$$\gamma = a_1 + \frac{a_2}{\varepsilon(\tau_{atm})\tau_{atm}} + \frac{a_3}{\varepsilon(\tau_{atm})}. \quad (24)$$

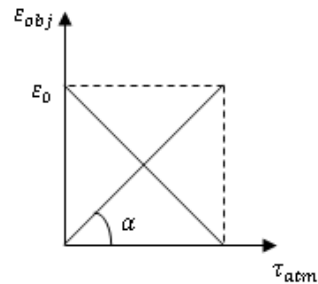


Fig. 3. Graphical representation of the model range (22) and (23), where $k = \arctg\alpha$

Taking into account the expressions (22)-(24) let's show that

$$\gamma_2 > \gamma_1, \quad (25)$$

where

$$\gamma_1 = a_1 + \frac{a_2}{(\varepsilon_0 - k\tau_{atm})\tau_{atm}} + \frac{a_3}{(\varepsilon_0 - k\tau_{atm})}, \quad (26)$$

$$\gamma_2 = a_1 + \frac{a_2}{k\tau_{atm}\tau_{atm}} + \frac{a_3}{k\tau_{atm}}. \quad (27)$$

Basic mathematical models (26) and (27) obtained at the model value $a_2 = a_3 = 1$; at $\tau_{atm} = (0.2 - 0.8)$. As can be seen from the graphs of the functions γ_1 and γ_2 (Fig. 4), the area under the curve of the function γ_2 is significantly larger than the curve under the graph of the function (1). This circumstance indirectly confirms the obtained result on the minimum of the objective function (13) in solutions (17) and (20).

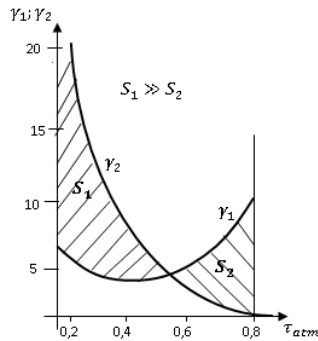


Fig. 4. Model graphs of functions γ_1 (26) and γ_2 (27)

Conclusions

A multi-radar extreme method for detecting a group of thermal flying objects using a group of ground-based IR radars is proposed.

It is shown that with a certain type of communication function between the emission coefficients of elements of a group of flying objects and the optical density of the atmosphere along the “object-radar” route, when a certain restrictive condition is imposed on this function, the total signal of the multi-radar complex reaches a minimum.

An approximate model confirmation of the workability of the proposed method has been obtained.

References

- [1] Modest M. F. (2013). *Radiative heat transfer*. Academic press: Waltham, Massachusetts, USA, 904 p., doi:10.1016/C2010-0-65874-3.
- [2] Gade R., Moeslund T. B. (2014). Thermal imaging cameras and their applications: a survey. *Machine Vision and Applications*, Vol. 25, pp. 245–262, doi:10.1007/s00138-013-0570-5.
- [3] Meola C. (2012). *Infrared Thermography Recent Advances and Future Trends*. Bentham Science Publishers, doi:10.2174/97816080514341120101.
- [4] Lahiri B., Bagavatiappan S., Jayakumar T., Philip J. (2012). Medical application of infrared thermography: A review. *Infrared Phys Technol*, Vol. 55, Iss. 4, pp. 221-235, doi: 10.1016/j.infrared.2012.03.007.
- [5] Becerra A. G., Holgin-Tiznado H. E., Garcia Alcaraz H. L., Camargo U. S., Garcia-Rivera B. R., Vardaska R. et al. (2021). Infrared thermal imaging monitoring of hands when performing repetitive tasks: An experimental study. *PLoS one*, Vol. 16, Iss. 5, e0250733, doi:10.1371/journal.pone.0250733.
- [6] Cruz-Vega I., Hernandez-Contreras D., Pergrina-Barreto H., Rangel J. D., Ramirez-Cortez J. M. (2020). Deep Learning Classification for Diabetic Foot Thermograms. *Sensors*, Vol. 20, Iss. 6, 1762; doi:10.3390/s20061762.
- [7] Kirimat A., Krejcar O., Selamat A., Herrera-Viedma E. (2020). FLIR vs SEEK thermal cameras in biomedicine: comparative diagnosis through infrared thermography. *BMC bioinformatics*, Vol. 21(Suppl 2):88. doi: 10.1186/s12859-020-3355-7.
- [8] Purohit R., Turner T. A., Pasco D. D. (2008). The use of infrared imaging in veterinary medicine. *In book: Medical Infrared Imaging. Principles and Practices*, pp. 31.1-31.8. Ed.: M. Diakides, J. D. Bronzino, D. R. Peterson, CRC Press. DOI:10.1201/9781420008340.ch21.
- [9] Dorea F. S., Vial F., Hammar K., Lindberg A., Lambrix P., Blomkvist E. et al. (2019). Drivers for the development of an Animal Health Surveillance Ontology (AHSO). *Prev Vet Med*, Vol. 166, pp. 39-48, doi:10.1016/j.prevetmed.2019.03.002.
- [10] Anagnostopoulos A., Barden M., Tulloch J., Williams K., Griffiths B., Bedford S., et al. (2021). A study on the use of thermal imaging as a diagnostic tool for the detection of digital dermatitis in dairy cattle. *J. Dairy Sci.*, Vol. 104(9), pp. 10194-10202, doi: 10.3168/jds.2021-20178.
- [11] Blel W., Hässig M., Kluzer F. (2021). Screening of feverish cows with a small portable infrared thermographic device. *Tierarztl Prax Ausg G Grosstiere Nutztiere*, Vol. 49, Iss. 1, pp. 12-20, doi: 10.1055/a-1307-9993, [Article in German].
- [12] Bogue, R. (2013). Sensors for condition monitoring: a review of technologies and applications. *Sensor Review*, Vol. 33, No. 4, pp. 295-299, doi:10.1108/SR-05-2013-675.
- [13] Alliot G. T., Higginson R. L., Wilcox G. D. (2023). Producing a thin coloured film on stainless steels – a review. Part 2: non-electrochemical and laser processes. *The International Journal of Surface Engineering and Coatings*, Vol. 101, Iss. 2, pp. 72-78, doi:10.1080/00202967.2022.2154495.
- [14] Huagang Liu, Wenxiong Lin, Minghui Hong. (2019). Surface coloring by laser irradiation of solid substrates. *APL Photonics*, Vol. 4, Iss. 5, doi:10.1063/1.5089778.
- [15] Al-Kassir A. R., Fernandez J., Tinaut F. V., Castro F. (2005). Thermographic study of energetic installations. *Applied Thermal Engineering*, Vol. 25, Iss. 2–3, pp. 183-190, doi:10.1016/j.applthermaleng.2004.06.013.
- [16] Sivasurian A., Vijayan D. S., Gorski V., Vodzi N., Vaverkova M. D., Koda E. (2021). Practical Implementation of Structural Health Monitoring in Multi-Story Buildings. *Buildings*, Vol. 11(6), 263; doi:10.3390/buildings11060263.
- [17] Falorka J. F., Miraltes J. P. N., Lanzinha J. K. G. (2021). New trends in visual inspection of buildings and structures: Study for the use of drones. *Open Engineering*, Vol. 11, Iss. 1, pp. 734-743, doi:10.1515/eng-2021-0071.
- [18] Khudov H., Yarosh S., Savran V., Zvonko A., Shcherba A., Arkushchenko P. (2020). The Technique of Research on the Development of Radar Methods of Small Air Objects Detection. *International Journal of Emerging Trends in Engineering Research*, Vol. 8, No. 7, doi:10.30534/ijeter/2020/132872020.
- [19] Kumari A., Kumar A., Reddy G. S. T. (2023). Performance analysis of the coherent FMCW photonic radar system under the influence of solar noise. *Front. Phys.*, Vol. 11, doi:10.3389/fphy.2023.1215160.

- [20] Marvasti F. S., Mosavi M. R., Nasiri M. (2018). Flying small target detection in IR images based on adaptive toggle operator. *IET Computer vision*, Vol. 12, Iss. 4, pp. 527-534, doi:10.1049/iet-cvi.2017.0327.
- [21] Bounaceur H., Khenchaf A., Le Caillec J.-M. (2022). Analysis of Small Sea-Surface Targets Detection Performance According to Airborne Radar Parameters in Abnormal Weather Environments. *Sensors*, Vol. 22(9):3263, doi: 10.3390/s22093263.
- [22] Smith T. M., Lakshmana V., Stumpf G. J., Ortega K. L., Khondl K., Cooper K. et al. (2016). Multi-Radar Multi-Sensor (MRMS) Severe Weather and Aviation Products: Initial Operating Capabilities. *Bulletin of the American Meteorological Society*, Vol. 97, Iss. 9, pp. 1617-1630, doi:10.1175/BAMS-D-14-00173.1.
- [23] Wang N., Zhang Y. (2015). A detection method for infrared multi-target in airspace background. *Proceedings of the SPIE*, Vol. 9795, id. 97951P 5 pp, DOI: 10.1117/12.2216079.
- [24] Güvenç İ., Ozdemir O., Yapici Y., Mehrpouyan H. and Matolak D. (2017). Detection, localization, and tracking of unauthorized UAS and Jammers. *201 IEEE/AIAA 36th Digital Avionics Systems Conference (DASC)*, pp. 1-10, doi: 10.1109/DASC.2017.8102043.
- [25] Quang Huy Tran, Dongyeob Han, Choonghyun Kang, Achintya Haldar, Jungwon Huh. (2017). Effects of Ambient Temperature and Relative Humidity on Subsurface Defect Detection in Concrete Structures by Active Thermal Imaging. *Sensors*, Vol. 17(8), 1718; doi:10.3390/s17081718.

Метод виявлення малих повітряних об'єктів, що з'являються в полі зору в контрольованій частині небесної сфери в інфрачервоному діапазоні

Агаєв Ф. Г., Асадов Х. Г., Алієва Г. В.

Стаття присвячена розробленому методу інфрачервоного виявлення групових віддалених високотемпературних об'єктів. Методом варіаційної оптимізації сформульовано та розв'язано задачу пошуку екстремуму сумарного інфрачервоного випромінювання групи неідентичних теплових об'єктів, які здійснюють груповий політ. Прикладами таких об'єктів є груповий політ літаків, наземні сцени з групою об'єктів, температурна діагностика різних точок будівель, контроль автомобільного руху на магістралях, контроль групових польотів птахів, дронів тощо. Визначено умову, за якої сумарне значення потоку інфрачервоного випромінювання теплових елементів у групі досягає екстремального значення. Розраховано функцію регресійної залежності між коефіцієнтом випромінювання теплових елементів групи та коефіцієнтом пропускання атмосфери. Задача оптимального керування хаотично розподіленими в атмосфері малими тепловими об'єктами практично вирішується за допомогою наземної мультирадіолокаційної системи, в якій елементи мультирадіолокаційної системи спостерігають літаючі об'єкти з різними значеннями коефіцієнта випромінювання на маршрутах і різною прозорістю атмосфери. Запропонований спосіб може бути використаний для дистанційного керування польотом або функціонуванням групи літаючих теплових об'єктів з різними значеннями коефіцієнта випромінювання зі спеціальною процедурою вибору керованого літака для спостереження елементом мультирадіолокаційної системи. Виявлено властивість екстремуму сумарного потоку ІЧ-випромінювання в оберненій залежності між коефіцієнтами випромінювання всіх керованих літаючих об'єктів і прозорістю атмосфери по маршруту між мультирадіолокаційним елементом і керованим літальним об'єктом.

Ключові слова: вимірювання температури; груповий політ; атмосфера; прозорість атмосфери